The *Modified*-Single Fiber Test: A Methodology for Monitoring Ballistic Performance

J. Kim, W. G. McDonough, W. Blair, G. A. Holmes

Polymers Division, National Institute of Standards and Technology, Gaithersburg, Maryland 20899-8541

Received 2 October 2006; accepted 11 January 2007
DOI 10.1002/app.27684
Published online 18 January 2008 in Wiley InterScience (www.interscience.wiley.com).

ABSTRACT: A minimally invasive testing methodology was developed to monitor the in-service performance of soft body armor. In the spirit of the single fiber test standard, ASTM C 1557-03, the fiber diameter was measured at five equally spaced locations along a 6-cm gauge length specimen. In addition, the single fiber test specimen was modified by placing reflecting tape just outside the specimen gauge length to allow the use of a laser extensometer for directly measuring fiber displacement and hence, strain. This modified testing methodology was found to be reproducible and provide data that was normally distributed based on descriptive statistics when variations in the fiber diameters along the length of the specimen were considered. The abnormality in the data, identified using Pierce's outlier criterion, may be associated with processing variations during the fiber manufacture and/or the woven fabrics and not associated with the testing methodology. Furthermore, the failure strain was found to be drastically reduced when the minimum fiber diameter along the length of the test specimen was less than 11 μm. This suggests that a methodology that accurately profiles fiber diameter changes along the gauge length of the fiber may be useful in analyzing single fiber test results. © 2008 Wiley Periodicals, Inc.* J Appl Polym Sci 108: 876–886, 2008

Key words: fibers; mechanical properties; single fiber test; ballistic performance

INTRODUCTION

The failure of a first responder's personal body armor composed of the ballistic fiber, poly(*p*-phenylene benzobisoxazole) (i.e., PBO) and the revelation that the President of the United States may have worn body armor utilizing this material prompted the National Institute of Standards and Technology Office of Law Enforcement and Standards (NIST-OLES) under the auspices of the National Institute of Justice (NIJ) to initiate a program to assess the long-term durability and effectiveness of current and future soft body armor products. In a recent review[1] of the potential degradation mechanisms of PBO fibers, ultraviolet (UV) exposure, exposure to moisture (associated with perspiration), elevated temperature exposure (resulting from storage of the device in the trunk of an automobile), and folding (associated with normal wear) have been identified as mechanisms that may compromise the structural integrity of the active ballistic fiber during use. A key part of the NIST-OLES research program requires the development of nondestructive performance test methods that link personal body armor performance to fundamental and measurable properties of the materials that are used in its construction. Since answers related to the long-term durability of the armor are sought, any testing methodology must allow for normal degradation mechanisms occurring under field conditions as well as controlled exposure conditions without compromising the structural integrity of the armor. As a result, the testing methodology must be non- or minimally-invasive to accurately determine the mechanical properties of the ballistic fibers, and the test results must correlate with the true ballistic performance properties of the armor.

By decoupling the ballistic impact of fiber properties from a principal vest construction parameter, areal density, Cunniff and Auerbach[2] empirically linked the performance of ballistic armor through the $(U)^{1/3}$ parameter, within the elastic limit, to the mechanical properties of the active fiber. The resulting equation, which has been recently supported by the theoretical work of Phoenix and Porwal,[3,4] is given below.

$$[U^*(m^3/s^3)]^{1/3} = \left[\frac{\sigma_f^u \varepsilon_f^u}{2\rho}\sqrt{\frac{E_{1f}}{\rho}}\right]^{1/3}$$

where m, denotes length in meters, s, denotes time in seconds, σ_f^u, is the fiber ultimate axial tensile strength, ε_f^u, is the fiber ultimate tensile strain, ρ, is the fiber density, and E_{1f}, is the longitudinal linear elastic fiber modulus.

Correspondence to: G. A. Holmes (gale.holmes@nist.gov).

Journal of Applied Polymer Science, Vol. 108, 876–886 (2008)

TABLE I
Theoretical Ballistic Performance of Common Fibers

Fiber	Density (Calc.) (ρ) (g/cm^3)	Strength (σ) (GPa)	Failure strain (ε) (%)	Modulus (E) (GPa)	$(U^*)^{1/3}$ (m/s)
PBO (as spun)	(1.56)	5.20	3.10	169	813
Spectra 1000	(0.97)	2.57	3.50	120	801
600 den. Kevlar KM2	(1.44)	3.40	3.55	82.6	682
850 den. Kevlar KM2	(1.44)	3.34	3.80	73.7	681
840 den. Kevlar 129	(1.44)	3.24	3.25	99.1	672
1,500 den. Kevlar 29	(1.44)	2.90	3.38	74.4	625
200 den. Kevlar 29	(1.44)	2.97	2.95	91.1	624
1,000 den. Kevlar 29	(1.44)	2.87	3.25	78.8	621
1,140 den. Kevlar 49	(1.41)	3.04	2.30	120	612
Carbon fiber	(1.80)	3.80	1.76	227	593
E-glass fiber	(2.89)	3500	4.70	74	559
M5 (2001 sample)	(1.74)	3.96	1.40	271	583
M5 Conservative	(1.70)	8.50	2.50	300	940
M5 Goal	(1.70)	9.50	2.50	450	1043

From this equation Cunniff has shown that the initial ballistic performance of PBO, if the areal density is held constant, exceeds that of other ballistic fibers such as poly(*p*-phenylene terephthalamide) (i.e., Kevlar), oriented ultra-high molecular mass polyethylene (i.e., Spectra), poly[2,6-diimidazo-(4,5-b:4′,5′-e) pyridinylene-1,4-(2,5-dihydroxy)phenylene] (i.e., PIPD or M5-current version), and S2 glass (see Table I). These data suggest that protective vests composed of PBO and Spectra 1000 fibers can be made 25% lighter than a corresponding Kevlar vest, while still providing the same ballistic protection[2] (i.e., flexible body armor). However, Spectra fibers, presumably because of their low-melting point, have not achieved the ballistic performance suggested by the Cunniff and Auerbach equation.[1] Irrespective of this anomaly, the equation has been shown to be useful in ranking the initial relative performance of most ballistic fibers.

If samples of the ballistic fiber can be obtained without compromising the vest, the above equation also suggests that the effectiveness of the vest can be monitored during use by developing a test methodology that accurately quantifies the modulus, strain-to-failure, and ultimate tensile strength of the active fiber. Since any long-term durability study may require repeated sampling from the same vest, the sample size and its relevance to the overall performance of the armor are critical issues that must be addressed. Two approaches that may be considered minimally invasive have been used to determine the mechanical properties of PBO fibers. These are the yarn tensile test (based on ASTM D 2256, JIS L-1013, and the research of Im et al.[5]) and the single fiber test (SFT) (based on the original ASTM standard for testing single fibers, D 3379-75). A comparative study[6] of these two methods using virgin PBO fibers revealed that the Young's modulus data from the two techniques are comparable, whereas, the ultimate tensile strengths obtained from the yarn tests are systematically lower than results from the SFT by 6 to 12% (see Table II).

The yarn test like the SFT involves deforming the specimens in tension until it breaks. Because uniform gripping of the individual fibers in a yarn is impossible, the methodology requires the twisting of the yarn to a specified twist per inch* that depends on the material to optimize load that is achieved prior to failure. Data from Im et al.,[5] shown in Figure 1 indicates that the tensile strength of virgin PBO fibers as measured by the yarn test increases through twisting by $\sim$ 25% up to 6 or 7 twists per inch without degrading the modulus. These researchers speculated that twisting, in this case, helps limit the effect of prematurely damaged fiber to local areas and lets the damaged fibers resume load-carrying capabilities away from those areas. When excessive twisting is applied, (above 7 twists per inch) both strength and modulus drop. These reductions are attributed to an increased fiber spiral angle as well as predamage on the fiber surfaces. Optical microscopy of the strand with 10 twists per inch, in its initial state prior to testing, revealed a large number of tensile cracks on the individual fiber surfaces that were generally perpendicular to the fiber axis. No other comparable data was found in the literature that correlates the effect of twists/inch with the properties of degraded PBO fibers. Therefore, the yarn test, although easy to perform, was not considered a suitable testing methodology due to the absence of data correlating the effect of twists/inch with the extent and type of degradation that may be experienced by the ballistic fibers.

The 2001 published report by Kitagawa et al.[6] of Toyobo, the manufacturer of PBO fibers, and the

*SI units are not used here since this is standard nomenclature for this industry.

TABLE II
Mechanical Properties of PBO Fiber Types

PBO fiber type	E (GPa)	σ_f^u (GPa)	ε_f^u (%)	Diameter (μm)	Reference
AS	91 ± 5	2.1 ± 0.3	4.3 ± 0.5	≈16	7
	180 ± 10	4.8 ± 0.6		12.3 ± 1.1	8
	173 ± 16.3	6.30 ± 0.88		11.9	6
	187	5.55		Yarn	6
HM	133 ± 11	2.2 ± 0.3	2.0 ± 0.3	≈16	7
	254 ± 19	5.5 ± 0.7		11.2 ± 1.0	8
	260 ± 24.4	5.90 ± 0.79		12	6
	258	5.59		Yarn	6
HM+	330 ± 30	5.4 ± 0.9		11.6 ± 1.2	8
	320 ± 29.7	5.10 ± 0.76		12.2	6
	352	4.72		Yarn	6

1992 and 2001 published reports by Young and coworkers[7,8] indicate that their preferred methodology for determining the single fiber properties of PBO fibers is based on the ASTM D 3379-75 testing standard. Jurisdiction of this standard was transferred in 1997 from ASTM committee D30 on High Modulus Fibers and Their Composites, to committee C28 on Advanced Ceramics. Largely through the Monte Carlo simulations performed by Lara-Curzio and Russ,[9] the ASTM D 3379-75 standard in 1998 was withdrawn in part because of technical inaccuracies associated with the use of the average of the cross-sectional area of several fibers for the calculation of individual fiber strengths.[10]

In August 2003, committee C28 published a new method (ASTM C 1557-03) for testing the tensile strength and Young's modulus of fibers, such as advanced ceramic, glass, carbon, aramid, and other fibers. The major changes/recommendations to the testing methodology of single fibers involved (a) a postmortem on the tested fiber to ascertain the fiber diameter in the plane where fracture occurred, (b) a relaxation of the ASTM D 3379-75 requirement that the minimum gauge length to be tested be 2000 times the nominal fiber diameter,[11,12] as long as gauge length dimensions are reported in conjunction with the single fiber test results, (c) retaining the compliance method for the indirect measure of strain, while inferring that optical strain flags placed along the gauge section of the fiber may provide a means of directly measuring the fiber strain, and (d) retaining the tab methodology for mounting single fiber specimens [see Fig. 2(a)], while allowing the direct gripping of large diameter fibers (>50 μm).

Since the primary objective of this research is to develop a testing methodology that accurately quantifies the change in properties of ballistic fiber during use, modifications to the procedure described in ASTM C 1557-03 were required to reflect issues that are unique to polymeric ballistic fibers. To understand the modifications that were made, it is worthwhile noting that early research on PBO fibers were conducted, with the exception of item (a) discussed earlier, in accordance with the new ASTM C 1557-03 standard. In this early research, Young and coworkers[6–8] applied the SFT methodology to assess the influence of processing conditions on the final material properties of PBO fibers. Stress–strain responses of ''as-spun" (AS), high-modulus (HM), and ultra high-modulus (HM+) PBO fibers are

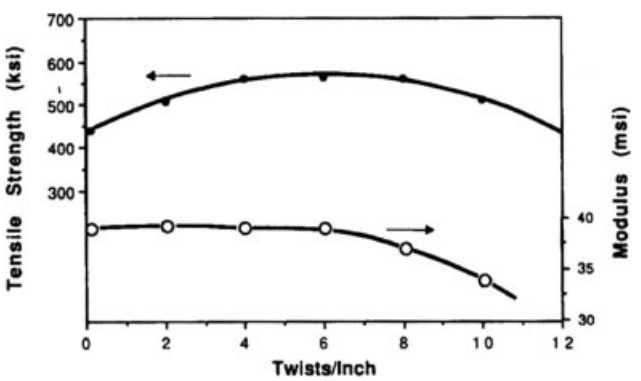

Figure 1 Dependence of tensile strength and modulus on twist/in for 130 denier yarns of PBO fibers. Data collected at 0.02/min strain rate and 5 in gauge length (Reproduced from Ref. 5, with permission from The Materials Research Society).

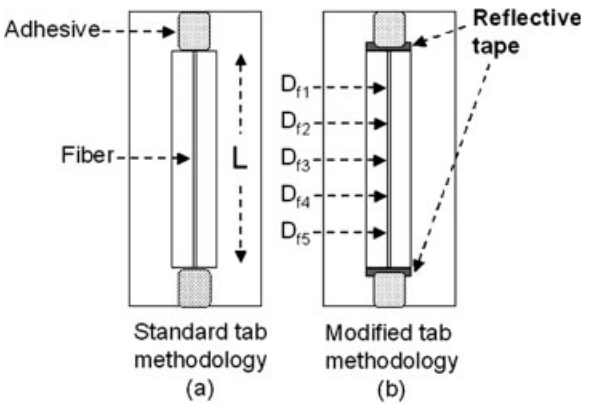

Figure 2 Modification made to tab methodology used in ASTM C 1557-03 test method.

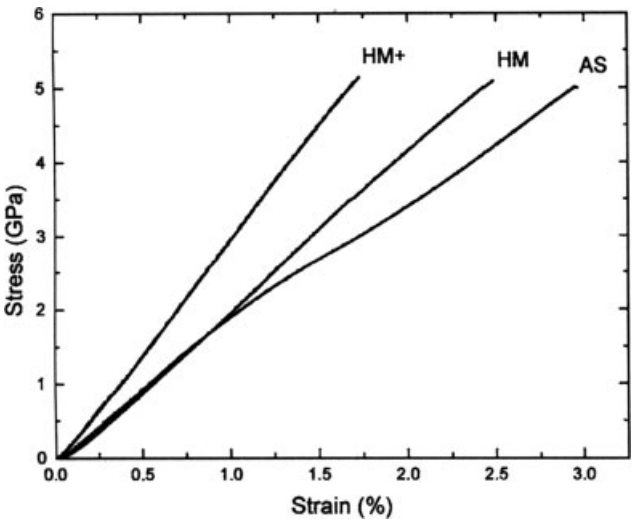

Figure 3 Typical stress/strain curves for AS, HM, and HM+ PBO fibers (Reproduced from Ref. 8, with permission from Springer).

shown in Figure 3, where the engineering stress is based on the average fiber diameter obtained from similar specimens in the bundle.

The production of the AS and HM fibers is thought to involve a dry-jet wet spinning process from air into an aqueous solution with the HM fiber given a subsequent heat treatment that improves the Young's modulus of the fiber. The HM+ fiber, whose stress–strain response is also shown in Figure 3, has a much high modulus than the AS and HM fibers. The fabrication of this fiber is believed to involve a nonaqueous spinning method. The pronounced knee in the stress strain curve of the AS-PBO fibers at $\sim$ 1.3% strain was reported in the 1992 research of Young and Ang[7] and the 2001 research of Davies et al.[8] A slightly different stress–strain curve was reported in the research of Kitagawa et al.[6] Kitagawa suggests that the difference in the stress–strain response between the AS and the HM fibers cannot be explained solely by an improvement in molecular orientation, and must be related to the existence of density fluctuations along the fiber axis. At these high-failure strains, it is probable that permanent deformation occurs in the PBO fibers, resulting in a distorted assessment of the fiber diameter at any fracture plane that may exist in the tested fiber. Furthermore, liquid nitrogen fracture surfaces by Adams et al.[13] showed fibrillation at a large scale (5–10 μm) and at a smaller scale (0.5–2 μm), with the smaller fibrils providing some connectivity between the larger fibrils. Heat treatment increased the tendency to fibrillate. Obviously, the postmortem recommended in ASTM C 1557-03 on the tested fiber to ascertain the fiber diameter in the plane where fracture occurs is not practical for ballistic fibers that undergo fibrillation during tensile failure.

Therefore in the spirit of the new standard for testing single fibers (ASTM C 1557-03), an alternative to the recommended postmortem approach is used. This approach because of the unique failure behavior of PBO fibers quantifies variations in the diameter along its length prior to testing. The impact of these fiber diameter variations on the mechanical properties of PBO fibers will be discussed.

Another technical barrier in developing this minimally invasive test is the precise determination of the strain-to-failure (ε_f^u), which also influences the longitudinal fiber modulus (E_{1f}). Therefore, the placement of strain tags (optical and reflective) on the tested fiber as discussed in ASTM C 1557-03 for use with a noncontact extensometer may be of critical importance. This is especially true if the tags significantly perturb the expected uniform strain field in the gauge section of the fiber to be tested and results in premature failure. To minimize the impact of the reflective tape that must be used with the laser extensometer in this report, the tape was placed just outside the gauge length of the test specimen [see Fig. 2(b)].

During the course of the review process for this manuscript, ASTM D 3822-01 was also suggested as an appropriate methodology for testing the PBO fibers investigated in this report. Indeed this standard, like ASTM C 1557-03, is recommended for testing aramid fibers, which are also used in soft body armor. However, ASTM D 3822-01 has as its core assumption, through the use of the centinewton per tex (cN/tex) or gram-force per denier (gf/den) measures for expressing the breaking tenacity, the fundamental assumption that the fiber has a uniform circular cross-section.[14] This in effect is the same fundamental assumption that led to the demise of ASTM D 3379-75. Furthermore, this assumption, at least for PBO fibers, is known to be incorrect from the test results of Young and coworkers,[8] who found standard deviations of ± 1 μm in the fiber diameter of each type of PBO fiber (i.e., AS, HM, and HM+). These researchers concluded that the large fiber diameter fluctuations were due to the fiber spinning process. Therefore, in the development of a testing methodology to monitor the properties of ballistic fibers as they are used and because the impact that these diameter fluctuations may have on a fiber's mechanical properties as it is degraded by environmental[1] or mechanical factors[15] is not known, ASTM C 1557-03 was modified as described earlier.

EXPERIMENTAL

Yarns of commercial poly(*p*-phenylene benzobisoxazole) fiber (PBO) were obtained from virgin material (i.e., materials not yet processed into body armor)

and from manufactured body armor that had been worn. The procedure for removing samples from existing body armor is described in the following paragraph.

A PBO fabric stack was removed from a lining inside of the body armor. Because the PBO fabric stack is interlocked together by stitching through the unit ply, the stitching thread was removed around the region targeted for yarn extraction in the PBO fabric stack. After removing the stitched thread from the vest, the layer of interest was collected from the PBO fabric stack. Yarns were then removed, beginning at the hem of the fabric and continuing toward the target region. The collected yarn was placed on a piece of aluminum foil with the ends held in place by removable tape. The foil was then folded lengthwise over the yarn to keep out light. The wrapped fibers were then placed in the drawer in a darkroom until harvesting. During the time the fibers were being harvested, mounted to the template, undergoing diameter measurements or tensile testing, they were exposed to only yellow frequency laboratory lighting that was free of UV frequencies. For fabricating a single fiber tensile test specimen, we manually separated a single fiber from a yarn and mount onto a paper template having a 6 cm $\times$ 1 cm rectangular window.

Fifty individual fibers, each $\sim$ 30–40 cm long, were obtained from a harvested yarn and mounted onto a paper tensile testing template. The template, printed on typical 21.6 cm (8.5 inch) by 27.9 cm (11 inch) printer paper that contained 1-cm major graduations and 1-mm minor graduations, held two or three rows of five fibers. Therefore, one fiber strand generated two or three test samples, each with a 6-cm gauge length. Individual fibers were initially attached temporarily to the paper template outside the region of the fiber that would undergo diameter measurement and tensile testing with double-sided tape (3M Stationary Products Division, St. Paul, MN 55119[†]). Prior to epoxy gluing, small strips ($\sim$ 1.2 cm $\times$ 0.2 cm) of silver reflective tape (supplied by United Calibration) were applied to the template at the top and bottom of the gauge section of each fiber sample. The reflective tape allows elongation measurements to be made by the United Calibration laser extensometer (Model EXT 62 LOE) while the sample is undergoing tensile testing. The fibers were then permanently bonded to the template by epoxy glue (Hardman Water-Clear Epoxy, Double/Bubble Green Package #04004). The epoxy glue was allowed to cover up to 0.1 cm thickness of the reflective tape to avoid the slip between fiber, paper template, and reflective tape.

Fiber diameters were measured using an optical micrometer (Excel Technologies, Model VIA-100) attached to a Nikon Optiphot-POL microscope equipped with a video camera (Optronix LX-450 RGB Remote Head microscope camera). The fiber image was viewed on a Sony PVM-1344Q color video monitor. The standard uncertainty in the diameter measurement of fiber diameters is 0.4 μm. All fiber samples had diameter measurements made at five equally spaced locations along the 6-cm gauge length. The five individual diameter measurements were averaged to give an average diameter value for each fiber sample (see Table IV). Between steps in the mounting, diameter measuring, and tensile testing processes, fiber samples were stored in the dark, in wooden map cabinets.

Although the compliance method in ASTM C 1557-03 has been found to be satisfactory for quantifying the properties of new fibers, the use of noncontact extensometers to detect gauge section elongation directly is often suggested[11,12] if a more accurate measure of strain is required, since specimen fragility prevents the use of normal strain-sensing devices, such as strain gauges, mechanical extensometers, etc. Consistent with this recommendation, a United Calibration Corporation Model EXT-62-LOE laser extensometer was used.

An initial gauge length of 5.1 cm or greater is required for optimum performance of the laser extensometer. Furthermore, because fiber strength is typically gauge length-dependent, a specimen length reflective of the amount of material that may be deformed during ballistic action is probably necessary, therefore a gauge length of 6.0 cm was chosen. The laser extensometer was calibrated using an Epsilon extensometer calibrator Model 3590C that has 10 cm of travel. A representative calibration curve is shown in Figure 4. The standard uncertainty in the strain at 6.1 cm associated with this measurement is 0.0001. The standard uncertainty in the load cell at 100 g is 0.001 g.

RESULTS AND DISCUSSION

Reproducibility of *modified*-SFT approach

To determine the reproducibility of this approach three sets of 50 specimens from a worn (W) vest were prepared by constructing 10 templates on (8½ by 11) in lined paper that contain three rows and five columns of open cavities with each gauge section being 6 cm in length. A yarn of PBO fibers, consisting of $\sim$ 330 fibers, was extracted from a worn vest. Fibers were then removed from the yarn and each fiber was mounted across the three open cavities

[†]Certain commercial materials and equipment are identified in this article to specify adequately the experimental procedure. In no case does such identification imply recommendation or endorsement by the National Institute of Standards and Technology, nor does it imply necessarily that the product is the best available for the purpose.

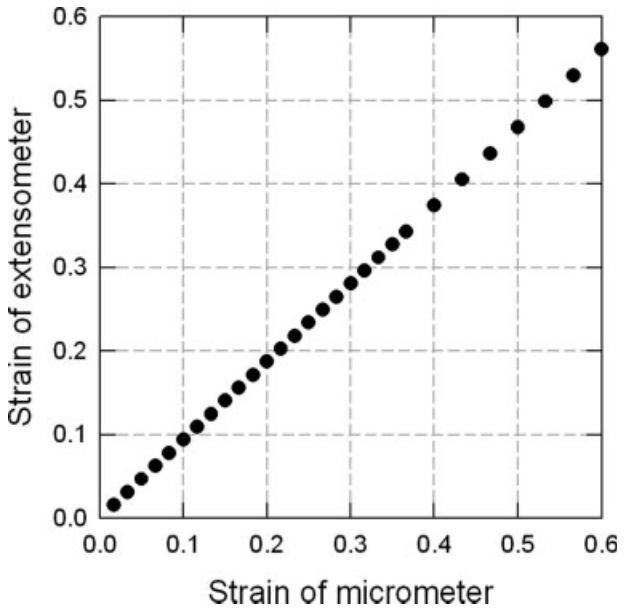

Figure 4 Calibration curve for the laser extensometer.

in each column, creating three sets of 50 fibers each whose properties should be equivalent.

Because the fiber diameter and strain-to-failure measurements are a departure from the ASTM D 3379-75 standard, the reproducibility of these measurements will be discussed initially. The ultimate tensile strength and the Young's modulus of the fiber sets will then be discussed since these values are derived from the measured load values, the fiber diameter measurements and the measured values of the displacement, whose values are used to derive measures of the strain.

Reproducibility of fiber diameter measurements

A summary of the data for the average fiber diameter of the W specimens in each set, labeled W_A, W_B, and W_C, is given in Table III, with the average fiber diameter of the 146 surviving specimens being (12.54 ± 0.53) μm, where the standard deviation reflects the average dispersion in the average fiber diameters calculated from the five individual measurements obtained on each fiber. The average fiber diameter is approximately the same size as the AS fiber diameters reported by Young et al. (see Table II) and about (7.0–7.5)% higher than the value derived from the denier and density values of PBO, which are taken to be 1.5 denier[16] and (1.54–1.56) g/cm^3,[2,16] respectively.[14] Analysis of variance (ANOVA) on the three sets showed that the average fiber diameters from each set were statistically indistinguishable (P-value = 0.696). The distributions were further analyzed for nonnormality by calculating the skewness (symmetry measure) and kurtosis (peakedness measure) with their respective standard errors. Using the accepted criteria that the skewness and kurtosis ratios should fall within −2 to +2 for a distribution to be considered normal, the kurtosis ratio of the W_A specimen set and the aggregate of all three data sets exhibited indications of nonnormality with values of 2.68 and 2.15, respectively (see Table III). These high values suggest that the tails of the distributions are longer than those of a normal distribution.[17]

Histograms of the distributions of the fiber diameters from the three sets are shown in Figure 5. To minimize the subjectivity involved in histogram construction and facilitate graphical comparisons, an optimal bin size (≈ 0.4 μm) for the histograms are shown in Figure 5. Figure 5 was obtained by averaging estimates from three methods specifically developed to optimize histogram bin size.[18–21] From Figure 5, the single data point (data point 4A) for the W_A specimen binned between 10.6 and 11 μm appears to be an outlier. A recalculation of the normality measures without this data point shows that

TABLE III
Statistical Analyses of Fiber Diameter Measurements

	Avg.	SD	Skewness	Std. Error	Skewness ratio	Kurtosis	Std. Error	Kurtosis ratio
Worn (W) fiber diameter statistics (μm)								
W_A No. 49	12.583	0.584	−0.400	0.340	−1.176	1.790	0.668	**2.680**
W_B No. 47	12.492	0.459	0.487	0.347	1.404	0.135	0.681	0.198
W_C No. 50	12.531	0.529	0.051	0.337	0.151	0.032	0.662	0.048
W_all – No. 146	12.536	0.525	−0.027	0.201	−0.075	0.858	0.399	**2.150**
Recalculation of non-normal distributions after removal of data point W_4A								
W_A No. 48	12.623	0.518	0.316	0.343	0.921	0.289	0.674	0.429
W_all No. 145	12.549	0.503	0.258	0.201	1.284	0.183	0.400	0.458
Virgin (V) fiber diameter statistics, μm								
V_A No. 50	12.640	0.550	1.115	0.337	**3.318**	5.494	0.662	**8.299**
V_B No. 50	12.478	0.497	0.511	0.337	1.516	−0.492	0.662	−0.743
V_all No. 100	12.559	0.527	0.887	0.241	**3.680**	3.080	0.478	**6.444**
Recalculation of non-normal distributions after removal of data point V_6A								
V_A No. 49	12.593	0.440	−0.571	0.340	1.679	−0.326	0.668	−0.488
V_all No. 99	12.535	0.470	0.027	0.243	0.111	−0.680	0.481	−1.413

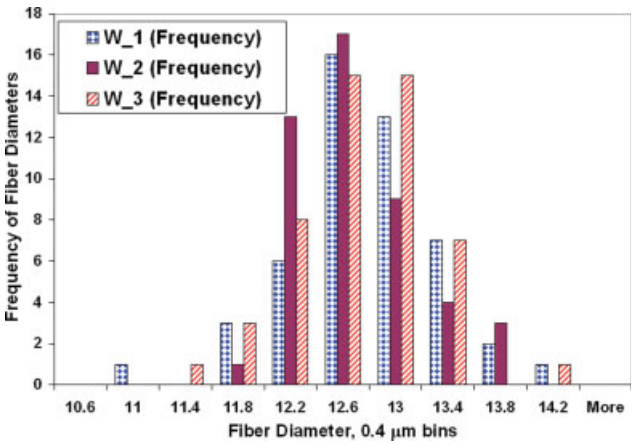

Figure 5 Distribution of measured fiber diameters from three sets of PBO fibers. [Color figure can be viewed in the online issue, which is available at www.interscience.wiley.com.]

the normality conditions are met for the W_A data set and the aggregate consisting of all three data sets (see Table III).

Although outlier rejection must be based on the physics of the measurement process, criteria such as Chauvenet or Peirce[22–25] can be used to provide a rational mathematical methodology for identifying outliers in a data set. The Peirce criterion suggests that data point 4A from distribution W_A, having an average fiber diameter of 10.654 μm, should be ignored (see histogram in Fig. 5). A recalculation of the W_A data without data point 4A (see Table III, W_A No. 48) brings the kurtosis ratio into normal range while keeping the skewness ratio within normal range. Furthermore, the removal of this single data point brings the kurtosis ratio of the overall distribution within normal range (see Table III, W_all No. 145).

However, since the fiber diameter values are averages of five measurements along its length, it is doubtful that the low value of the 4A data point can be attributed to measurement errors. A detailed investigation of the five measurements made along each fiber length indicated that 3 of the 146 sets of fiber diameters (4A, 31A, and 49C) exhibited standard deviations of the five averaged fiber diameter values that were much higher than the overall population. The fiber diameter measurements made along the length of these three questionable specimens are shown in Table IV along with the samples that complete the set, since the A, B, and C samples were obtained from the same fiber filament. For comparison to a typical specimen set, the ABC specimens from the W_17 set are also provided. In two of the three specimens, W_4A and W_49C, that exhibited a large standard deviation, multiple low-adjacent measurements were made along the fiber suggesting that the recorded change in diameter is real rather than due to a measurement error. This suggests that the diameters of the fibers from the W vest are only nominally uniform, with $\sim$ 2.1% of the test specimens or $\sim$ 10% of the fibers yielding erratic changes in diameter along their length.

Finally, two sets of 50 specimens were prepared from virgin (V) fiber material. The two average fiber diameter populations from the V fibers when compared with the three sets of W vest specimens were found to be statistically indistinguishable by ANOVA at the 95% confidence level (*P*-value of 0.537). Since all the populations are averages of five measurements, the population of minimum and maximum values from each measurement set was checked for consistency. For the W vest the three sets of minimum and three sets of maximum values were indistinguishable at the 95% confidence level with *P*-values of 0.870 and 0.733, respectively. Inconsistency was observed in the V fibers where *P*-values of 0.585 and 0.013 were obtained for the minimum and maximum values, respectively. Since the A and B samples from the V-fibers were obtained from the

TABLE IV
Fiber Diameter Measurements from Selected Single Fiber Specimens

Specimen	Measurement number (values in μm) 1	2	3	4	5	Average (μm)	SD (μm)
W_4A	13.56	**7.10**	**10.01**	**10.01**	12.59	10.65	**2.53**
B	12.91	12.91	11.62	11.62	12.91	12.39	0.71
C	13.56	11.94	12.27	13.23	12.91	12.78	0.67
W_31A	**9.04**	11.30	12.91	12.91	13.56	11.94	**1.83**
B	12.91	12.91	11.62	13.56	12.59	12.72	0.71
C	11.30	12.59	12.91	12.27	11.62	12.14	0.67
W_49A	12.91	12.59	10.98	11.94	10.98	11.88	0.89
B	11.30	12.91	11.62	13.56	12.27	12.33	0.92
C	**9.04**	**8.39**	13.56	12.59	12.59	11.23	**2.34**
W_17A	13.56	11.94	11.62	12.27	12.59	12.40	0.74
B	12.27	13.23	12.27	13.23	12.59	12.72	0.49
C	11.62	12.91	11.62	13.23	12.59	12.39	0.74

TABLE V
Strain to Failure Analyses

	Avg.	SD	Skewness	Std. Error	Skewness Ratio	Kurtosis	Std. Error	Kurtosis Ratio
Strain to failure								
W_A No. 46	0.01977	0.0035	−1.531	0.350	**−4.374**	3.221	0.688	**4.682**
W_B No. 44	0.01913	0.0032	−1.948	0.357	**−5.457**	5.091	0.702	**7.252**
W_C No. 48	0.01883	0.0037	−1.309	0.343	**−3.816**	2.954	0.674	**4.383**
W_all No. 138	0.01924	0.0035	−1.497	0.206	**−7.267**	3.199	0.410	**7.802**
Strain to failure with suspect data points removed								
W_A No. 44	0.02028	0.0026	−0.536	0.357	−1.501	−0.079	0.702	−0.113
W_B No. 42	0.01966	0.0021	−0.534	0.365	−1.463	−0.038	0.717	−0.053
W_C No. 46	0.01934	0.0028	−0.238	0.350	−0.680	0.195	0.688	0.283
W_all No. 132	0.01976	0.0025	−0.399	0.211	−1.891	0.057	0.419	0.136

same fiber filament the inconsistency in the maximum values indicates statistically significant variation in the fiber diameter along the length of a given fiber.

The populations of minimum fiber diameters from the V- and W-fiber sets were indistinguishable (*P*-value of 0.625). Since the two populations of maximum fiber diameters for the V-fibers were distinguishable at the 95% confidence level each set was compared with the maximum fiber diameters from the three indistinguishable sets of W-fibers, and found to be indistinguishable and distinguishable with *p*-values of 0.862 and 0.023 for the V_A and V_B samples, respectively. Therefore, variations in the fiber diameter were observed in worn and virgin PBO fibers.

Reproducibility of strain-to-failure measurements

Of the 146 specimens, 138 specimens were tested successfully using the *modified*-SFT approach. The strain-to-failure values are shown in Table V. In each specimen set, the skewness ratio and kurtosis ratio suggests a nonnormal distribution. Recalling, that the high kurtosis values suggests that the tails of the distributions are longer than those of a normal distribution,[17] a histogram of the combined data sets (see Fig. 6) shows a bimodal distribution of 132 specimens and six specimens with the failure strain of the latter being below 1.0%.

The six data points below 1.0% (W_4A, W_6A, W_26B, W_35B, W_5C, and W_6C) can be eliminated using Peirce's criterion. Note that in the previous section, the W_4A, which had a strain-to-failure of 7.6%, was found to have a small-average fiber diameter along its length with an abnormally large standard deviation, reflective of the large variation in fiber diameters measured along the 6-cm gauge length of the specimen (see Table IV). Of the remaining five specimens, W_5C (ε_f = 0.006316) and W_6C (ε_f = 0.007612) each had at least one fiber diameter measurement along its length less than 10.50 μm. To better quantify the impact of the fiber diameter reduction on the strain-to-failure behavior, the failure strain of each specimen was plotted with respect to the smallest of the five-fiber diameter measurements made along its length (see Fig. 7).

In Figure 7, the data is divided into eight groups. Six of these groups display variations in strain measurements at a single minimum fiber diameter. The strain-to-failure data of all specimens with at least one measured fiber diameter below 11.0 μm were grouped together, and a final group was made combining all fibers whose minimum fiber diameter was 12.9 μm or larger. ANOVA on the seven groups whose minimum fiber diameter was at least 11.0 μm showed that these groups were statistically indistinguishable (*P*-value of 0.520). Inclusion of the strain-to-failure data for specimens, whose minimum fiber diameter is below 11.0 μm, shows that this group is statistically distinguishable from the other seven

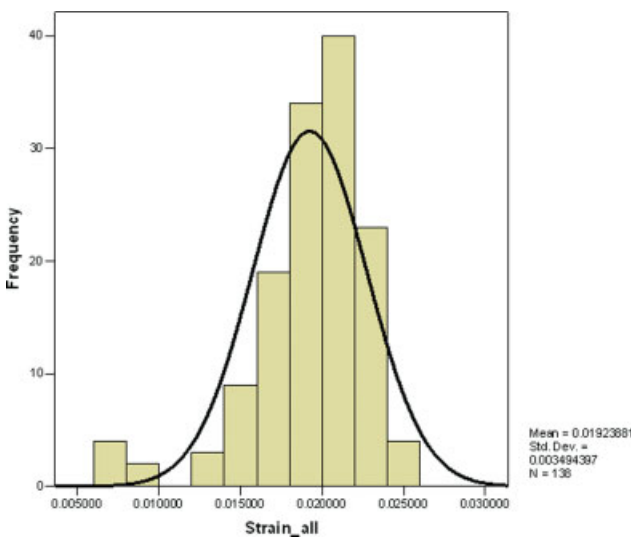

Figure 6 Histogram plot of strain-to-failure values obtained from the single fiber test of PGC L5-S1 specimens. [Color figure can be viewed in the online issue, which is available at www.interscience.wiley.com.]

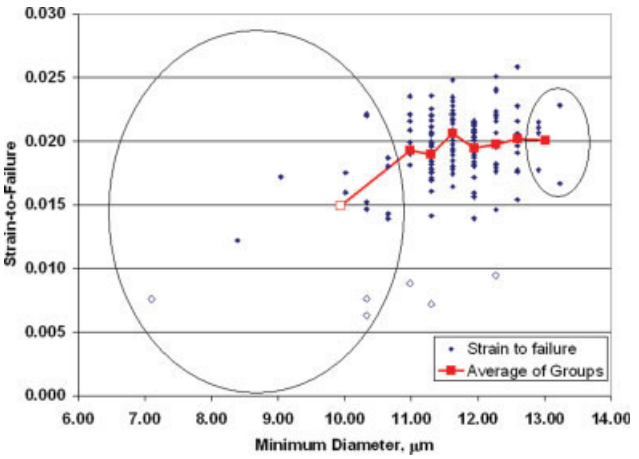

Figure 7 Strain-to-failure of single fiber test specimens plotted against the minimum fiber diameter measured along its 6-cm gauge length. The average strain to failure with respect to the minimum fiber diameter was plotted by dividing the 138 data points into eight groups. The data within the two circles constitute two separate groups containing data from multiple minimum fiber diameters, while all other data was grouped according to a single minimum fiber diameter. [Color figure can be viewed in the online issue, which is available at www.interscience.wiley.com.]

groups with a *P*-value of 3.61 E-05. Furthermore, the data indicates that one can expect 2.5% of the specimens to have a strain-to-failure less than or equal to 1.0% if the minimum fiber diameter along the specimen gauge length is 11.0 μm or greater. This expectation, however, increases to 20% if the minimum fiber diameter along the specimen gauge length is less than 11.0 μm along with an average drop in the fiber's failure strain of 25%.

Consistent with these results, the W_31A and W_49C specimens, mentioned in the previous section (see Table IV), also exhibited large variations in the fiber diameter measurements along their lengths and yielded strain-to-failure values of 1.72 and 1.22%, respectively. Although neither specimen's elimination could be justified, the strain-to-failure of the W_49C specimen was the 7th lowest value and just inside the acceptable tail for a Gaussian distribution. The strain-to-failure of the W_31A specimen was also on the low side relative to the revised average strain-to-failure (i.e., using the 132 specimens), being just outside of one standard deviation from the revised mean. A check of the fiber diameter data also reveal that any specimen with a least one fiber diameter measurement below 11.0 μm also exhibits a strain-to-failure below 1.76%, with these data including four of the remaining five specimens that were also eliminated by the Peirce Criterion.

These analyses and results suggest that small fiber diameter measurements along the length of the specimen promote premature failure of the specimen as reflected in the strain-to-failure measurement. By eliminating the six data points below 1.0% strain, the remaining data yielded a combined distribution and individual distributions that fall within the normality criteria defined earlier (see Table V).

Reproducibility of ultimate tensile strength measurements

Using these remaining 132 specimens and the new methodology for measuring the fiber diameters, the ultimate tensile strength and modulus of the fibers from the worn vest (W) are given in Table VI. Each

TABLE VI
Ultimate Tensile Strength and Modulus Analyses

	Avg.	SD	Skewness	Std. Error	Skewness Ratio	Kurtosis	Std. Error	Kurtosis Ratio
Ultimate tensile strength (GPa)								
W_A No. 44	2.597	0.345	−0.700	0.357	−1.96	0.423	0.702	0.60
W_B No. 42	2.556	0.287	−0.720	0.365	−1.97	0.254	0.717	0.35
W_C No. 46	2.519	0.364	−0.367	0.350	−1.05	0.358	0.688	0.52
W_all No. 132	2.557	0.334	−0.557	0.211	**−2.64**	0.320	0.419	0.76
Ultimate tensile strength minus data points 21A, 17B, and 49C (GPa)								
W_A No. 43	2.618	0.320	−0.561	0.361	−1.55	0.293	0.709	0.41
W_B No. 41	2.576	0.260	−0.447	0.369	−1.21	−0.508	0.724	−0.70
W_C No. 45	2.538	0.345	−0.261	0.354	−0.74	0.425	0.695	0.61
W_all No. 129	2.576	0.311	−0.413	0.213	−1.94	0.245	0.423	0.58
Modulus (GPa)								
W_A No. 43	136.41	11.12	−0.005	0.361	−0.014	−1.220	0.709	−1.721
W_B No. 41	137.63	9.81	0.173	0.369	0.469	−0.379	0.724	−0.523
W_C No. 45	142.18	13.51	0.259	0.354	0.732	−0.164	0.695	−0.236
W_all No. 129	138.81	11.82	0.307	0.213	1.441	−0.124	0.423	−0.293
Modulus minus 11A data point (GPa)								
W_A No. 42	135.15	12.82	−0.322	0.361	−0.892	−0.727	0.709	−1.025
W_B No. 41	137.01	10.56	−0.131	0.365	−0.359	0.121	0.717	0.169
W_C No. 45	141.07	15.14	−0.154	0.350	−0.440	0.036	0.688	0.052
W_all No. 128	137.83	13.19	−0.073	0.212	−0.344	0.029	0.420	0.069

ultimate tensile strength (UTS) distribution exhibits normality, however, the combined UTS distribution of all 132 test-specimens exhibits nonnormality in the skewness ratio with a value of −2.64. Applying Peirce's Criterion to the individual data sets suggested the elimination of data point 21A (UTS = 1.704 GPa, minimum fiber diameter of 10.7 μm) and data point 17B (UTS = 1.749 GPa, minimum fiber diameter of 12.3 μm). Although the A, B, and C data sets for the UTS were statistically indistinguishable at the 95% confidence level with a *P*-value of 0.540, the larger standard deviation in the C data set (see Table VI) precluded the statistical elimination of the 49C data point (UTS = 1.670 GPa) even though its UTS is lower than 21A and 17B and it has a minimum fiber diameter of 8.4 μm (see Table IV). Since the high negative value in the combined data set indicates a long left tail, data point 49C is also eliminated to bring the combined data set into normality. The statistical analyses of the resulting 129 data points and the individual data sets reduced by one specimen each are given in Table VI. Note that, two of the three additional data points that were eliminated are also associated with the nonuniformity of the fiber along its length.

Reproducibility of the Young's modulus

Since the modulus data is obtained from the slope of the stress–strain curve one would not expect that specimens that exhibited premature failure to also exhibit a faulty modulus. However, to be consistent, the modulus data that corresponds to the six specimens that exhibited premature failure were excluded from analysis. With these deleted specimens, the W data sets were indistinguishable at the 95% confidence level with a *P*-value of only 0.0528. Further analysis showed that the W_A data set was distinguishable from the W_C data set with a *P*-value of 0.0312, while W_A and W_B were indistinguishable ($\alpha = 0.05$) with a *P*-value of 0.594. These analyses suggest a slight stiffening of the fiber modulus at the lower part of the vest near the waist relative to the portion of the fiber near the chest. Further analyses will be needed to confirm these results and determine the potential source of this increase, however, it should be noted that tension and heat are used to increase the modulus of HM and HM+ fibers relative to the AS fibers that are used ballistic vest construction. It is worthwhile noting that the strain-to-failure averages although statistically indistinguishable at the 95% confidence trends toward lower values from the W_A distribution to the W_C distribution (see Table V). This latter result is consistent with the property changes observed between AS and HM fibers. The modulus distributions were found to be normal with respect to the skewness and kurtosis ratios (see Table VI).

Finally, the lower modulus values obtained in this report for PBO relative to published values (see Table I) are at least in part related to the average measured fiber diameter values ($\approx$ 12.55 μm) used in this report to calculate the fiber stress. Using the denier and density of PBO, the fiber diameter is estimated to be $\sim$ 11.8 μm. Correcting for this difference the average moduli values for the W_A, W_B, and W_C specimens are 156 ± 13, 154 ± 14, and 163 ± 17 GPa, respectively, with the average for the population being 158 ± 15 GPa.

CONCLUSIONS

In an effort to develop a minimally invasive testing methodology for monitoring the in-service performance of soft body armor, the ASTM C 1557-03 standard was modified by measuring the fiber diameter at five equally spaced locations along a 6-cm gauge length specimen, while specimen construction was modified by placing reflecting tape just outside of the gauge section to allow the use of a laser extensometer for directly measuring fiber displacement and hence, strain. The five equally spaced fiber diameter measurements were averaged and used to calculate the stress in each individual fiber during testing.

To test the reproducibility of this modified methodology, 50 ballistic fibers were extracted from a yarn obtained from a worn vest. Each fiber was stretched across three cavities in a template, thereby making three identical sets of 50 specimens. These three sets of fibers were randomly tested and the output results were evaluated for reproducibility and nonnormality using Peirce's Criterion for outlier detection, ANOVA, and descriptive measures of distribution properties.

Although the three average sets of fiber diameters were statistically indistinguishable at the 95% confidence level, nonnormality in the average fiber diameter measurements were detected and traced to variations in the fiber diameter along the length of the specimen. These variations were found to generally result in premature failure (below 1% strain) of the fiber specimen when one of the five fiber diameter measures was below 11.0 μm. These experimental results support the Monte Carlo simulations performed by Lara-Curzio and Russ,[9] and indicate that a methodology that accurately profiles fiber diameter changes along the gauge length of the fiber may be useful in analyzing single fiber test results from fibers that undergo fibrillation during tensile fracture.

Furthermore, the small fiber diameter measurements along the fiber length also influenced the statistical distribution of the ultimate tensile strength determinations. After removal of these abnormalities, the triplicate sets of samples were found to be indistinguishable with respect to all parameters needed to quantify ballistic performance. These results suggest that the modified ASTM C 1557-03 testing methodology provides a quantitative approach for monitoring changes in ballistic fiber properties.

References

1. Holmes, G. A.; Rice, K.; Snyder, C. R. J Mater Sci 2006, 4105.
2. Cunniff, P. M.; Auerbach, M. A. 23rd Army Science Conference, Assistant Secretary of The Army (Acquisition, Logistics And Technology), Orlando, Florida, December 2002.
3. Phoenix, S. L.; Porwal, P. K. Int J Solids Struct 2003, 40, 6723.
4. Phoenix, S. L.; Porwal, P. K. Int J Fract 2005, 135, 217.
5. Im, J.; Percha, P. A.; Yeakle, D. S. Materials Research Society Symposium Proceedings; The Materials Research Society: Warrendale, PA, 1988; p 307.
6. Kitagawa, T.; Yabuki, K.; Young, R. J. Polymer 2001, 42, 2101.
7. Young, R. J.; Ang, P. P. Polymer 1992, 33, 975.
8. Davies, R. J.; Montes-Moran, M. A.; Riekel, C.; Young, R. J. J Mater Sci 2001, 36, 3079.
9. Lara-Curzio, E.; Russ, C. M. J Mater Sci Lett 1999, 18, 2041.
10. Lara-Curzio, E.; Garcia, D. Jr. Ceram Eng Sci Proc 2001, 22, 363.
11. Whitney, J. M.; Daniel, I. M.; Pipes, R. B. Experimental Mechanics of Fiber Reinforced Composite Materials; The Society for Experimental Stress Analysis (SESA): Brookfield Center, CT, 1982; Vol. 4, p 151.
12. Committee D-20 On Plastics; Committee D-30 On High-Modulus Fibers And Their Composites, Plastics. Materials, Film, Reinforced and Cellular Plastics; High Modulus Fibers and Composites; American Society for Testing And Materials: Philadelphia, PA., 1980; p 856.
13. Adams, W. W.; Grieshop, T.; Helminiak, T.; Hunsaker, M.; O'brien, J. F.; Altieri, M.; Bai, S. J.; Brandt, A. V.; Frantini, A. V.; Hwang, W.-F.; Price, G. E.; Soloski, E.; Haddock, T.; Krause, W. J.; Lenhert, P. G. Processing, Properties, Structure, and Morphology of Pbo and Abpbo Polymer Fibers; Afwal-Tr-86-4011/Adb109981; Materials Laboratory, Air Force Wright Aeronautical Laboratories, Wright-Patterson Air Force Base, Ohio, August 1986.
14. Doguc, N. B.; Seyam, A. M.; Oxenham, W. Int Nonwovens J 2004, 13, 48.
15. Kim, J. H.; Brandenburg, N.; Mcdonough, W.; Blair, W.; Holmes, G. A., J Appl Mech, to appear.
16. Toyobo, L. Toyobo Zylon Pbo-Hm Poly(P-Phenylene-2,6-Benzobisoxazole) Fiber; Toyobo: Japan, 2006.
17. SPSS. SPSS Base 8.0 Applications Guide, SPSS: Chicago, 1998; p 27.
18. Scott, D. W. Biometrika 1979, 66, 605.
19. Freedman, D.; Diaconis, P. Z Wahrsch V Gebiete 1981, 57, 453.
20. Freedman, D.; Diaconis, P. Z Wahrsch V Gebiete 1981, 58, 139.
21. Hoaglin, D. C.; Mosteller, F.; Tukey, J. W. Understanding Robust and Exploratory Data Analysis; Wiley: New York, 1983; p 25.
22. Taylor, J. R. An Introduction to Error Analysis: The Study of Uncertainties in Physical Measurements; University Science Books: Sausalito, CA, 1997; p 166.
23. Bevington, P. R.; Robinson, D. K. Data Reduction and Error Analysis for the Physical Sciences; McGraw-Hill: Boston, MA, 1992; p 58.
24. Ross, S. M. J Eng Technol 2003, 20, 31.
25. Chauvenet, W. A Manual of Spherical and Practical Astronomy, 1st ed.; Lippinincott: Philadelphia, 1863; Reprint-Dover Publications: New York, 1960.